ARTICLE
Life Research 2026;9(1):2. https://doi.org/10.53388/LR20260002

A bacterial type-II toxin-antitoxin-mediated gene amplification system in *Saccharomyces cerevisiae*

Samuel Evans[1, 2], Zeyu Lu[1, 2, 3], Liam McDonnell[1, 2], Will Anderson[3], Francisco Peralta[1, 2], Tyson Watkins[1, 2], Hafna Ahmed[4], Carlos Horacio Luna-Flores[2], Thomas Loan[5], Laura Navone[2], Matt Trau[3, 6], Colin Scott[4, 7], Robert E. Speight[1, 2, 8], Claudia E. Vickers[1, 2], Bingyin Peng[1, 2, 3*]

[1]ARC Centre of Excellence in Synthetic Biology, Queensland University of Technology, Brisbane 4000, Australia.
[2]Centre of Agriculture and the Bioeconomy, School of Biology and Environmental Science, Faculty of Science, Queensland University of Technology, Brisbane 4000, Australia.
[3]Australian Institute for Bioengineering and Nanotechnology, The University of Queensland, Brisbane 4072, Australia.
[4]CSIRO Environment, Black Mountain Science and Innovation Park, Canberra 2601, Australia.
[5]CSIRO Agriculture & Food, Black Mountain Science and Innovation Park, Canberra 2601, Australia.
[6]School of Chemistry and Molecular Biosciences, the University of Queensland, Brisbane 4072, Australia.
[7]School of Molecular Sciences, The University of Western Australia, Perth 6009, Australia.
[8]Advanced Engineering Biology Future Science Platform, Commonwealth Scientific and Industrial Research Organisation (CSIRO), Black Mountain 2601, Australia.

[*]**Correspondence to:** Bingyin Peng, Australian Institute for Bioengineering and Nanotechnology, The University of Queensland, Corner College and Cooper Rds, Brisbane 4072, Australia. E-mail: bingyin.peng@yahoo.com.

Abstract

Background: Tandem gene repeats naturally occur as important genomic features and determine many traits in living organisms, like human diseases and microbial productivities of target bioproducts. **Methods:** Here, we developed a bacterial type-II toxin-antitoxin-mediated method to manipulate genomic integration of tandem gene repeats in *Saccharomyces cerevisiae* and further visualised the evolutionary trajectories of gene repeats. We designed a tri-vector system to introduce toxin-antitoxin-driven gene amplification modules. **Results:** This system delivered multi-copy gene integration in the form of tandem gene repeats spontaneously and independently from toxin-antitoxin-mediated selection. Inducing the toxin (RelE) expressing *via* a copper (II)-inducible *CUP1* promoter successfully drove the *in-situ* gene amplification of the antitoxin (RelB) module, resulting in ~40 copies of a green fluorescence reporter gene per copy of genome. Copy-number changes, copy-number increase and copy-number decrease, and stable maintenance were visualised using the green fluorescence protein and blue chromoprotein AeBlue as reporters. Copy-number increases happened spontaneously and independent on a selection pressure. Increased copy number was quickly enriched through toxin-antitoxin-mediated selection. **Conclusion:** In summary, the bacterial toxin-antitoxin systems provide a flexible mechanism to manipulate gene copy number in eukaryotic cells and can be exploited for synthetic biology and metabolic engineering applications.

Keywords: tandem repeats; gene amplification; toxin-antitoxin; genetic dosage; genome evolution

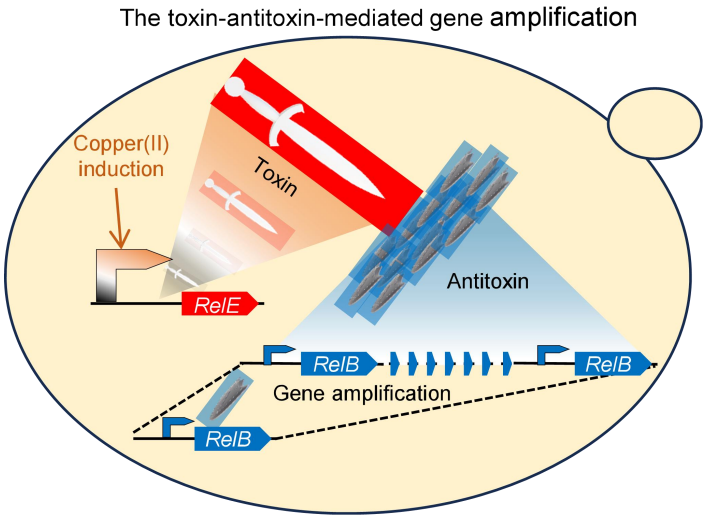

Author contributions

Samuel Evans, conceptualization, methodology, investigation, data analysis, writing—original draft. Zeyu Lu, Liam McDonnell, Will Anderson, Francisco Peralta, and Tyson Watkins, methodology, investigation. Hafna Ahmed, Carlos Horacio Luna-Flores, Thomas Loan, and Laura Navone, conceptualization, data analysis. Matt Trau and Colin Scott, resources. Robert E. Speight funding acquisition, project administration. Claudia E. Vickers, funding acquisition. Bingyin Peng, conceptualization, methodology, investigation, data analysis, writing—original draft, and writing—review & editing.

Competing interests

Authors declare no competing interests.

Acknowledgments

This research was supported partially by the Australian Government through the Australian Research Council Centres of Excellence funding scheme (project CE200100029). The views expressed herein are those of the authors and are not necessarily those of the Australian Government or Australian Research Council. This work is supported by Galaxy Australia, a service provided by the Australian Biocommons and its partners.

Abbreviations

rDNA, ribosomal RNA genes; *S. cerevisiae*, *Saccharomyces cerevisiae*; YIp, yeast integrative plasmid; *E. coli*, *Escherichia coli*; Hph, hygromycin B phosphotransferase; yEGFP, yeast-enhanced green fluorescent protein; YPD, yeast extract-peptone-dextrose; PCR, polymerase chain reaction; YNB, yeast nitrogen base; ToxAmp, toxin-antitoxin-mediated gene amplification; AeBlue, Blue chromoprotein from *Actinia equina*.

Citation

Evans S, Lu Z, McDonnell L, et al. A bacterial type-II toxin-antitoxin-mediated gene amplification system in *Saccharomyces cerevisiae*. *Life Res.* 2026;9(1):2. doi: 10.53388/LR20260002.

Peer review information

Life Research thanks Cheng-Gong Liu and other anonymous reviewers for their contribution to the peer review of this paper.

Editorial Advisory Board: Nguyen Hoang Loc.

Executive editor: Xin-Yun Zhang.

Received: 14 September 2025; **Revised:** 21 November 2025; **Accepted:** 31 December 2025; **Available online:** 04 January 2026.

Introduction

Tandem gene repeats, in the form of an array of two or more copies of a gene, commonly exist in cell genomes, i.e., ribosomal RNA genes (rDNA) [1–3], oncogenic genes [4], drug resistant genes [5–7], secondary metabolite biosynthetic genes [8, 9], and many other trait genes [10–12]. Their occurrence is generally regarded as the result of gene amplification, which increases gene copy number (gene dosage) and provides a phenotypic advantage during natural or artificial selection [5, 7, 8]. Manipulating tandem gene repeats has been used for optimising bioproduction of small-molecular metabolites and proteins in metabolic engineering and synthetic biology [13–16]. Examining tandem gene repeats is an important method in understanding the development of relevant genetic diseases in humans [4]. Genetic manipulation methods have therefore been developed towards precise manipulation and examination of gene tandem repeats [13, 17].

In the yeast *Saccharomyces cerevisiae* (*S. cerevisiae*), tandem gene repeats and gene amplification have been investigated and engineered in a variety of studies. For example, rDNA repeats are used in understanding cell aging [18]. Using the copper resistance *CUP1* gene as an example, elevated Cu^{2+} levels can drive the amplification of the *CUP1* gene, which relates to transcription-mediated DNA replication stalling [19]. In metabolic engineering and synthetic biology, multi-copy integration of transgenes in form of tandem repeats is a common engineering strategy to increase protein expression levels [17, 20]. It has been shown that the formation of a long tandem gene array in yeast genome through the yeast integrative plasmids [21, 22]. In these plasmids, either an auxotrophic marker or a dominant resistant marker is used for plasmid maintenance or selection of clones with increased copy number [16, 23–26]. The tandem amplification of xylose and cellobiose utilization genes has also been seen during prolonged adaptive growth [27–29]. The gene amplification in these cases is selectable due to the growth advantage of increased gene dosages. In consistent with this principle, we use the haploinsufficient genes as the selectable marker to drive the gene amplification by weakening their expression dosage per gene copy. This resulted in gene amplification up to ~50 copies of transgenes. Furthermore, the multi-copy integration in form of tandem gene repeats occurred randomly as the result of the transformation of a yeast integrative plasmid (YIp) and independent of the growth-related selection pressure [30].

Additionally, in bacteria and archaea, the toxin-antitoxin systems can be employed to maintain genome stability and control gene copy number [31–33]. The toxin-antitoxin systems contain two modules: a toxin module functioning as a killing or growth-inhibiting mechanism in the host cell and its antidote, the antitoxin module [32, 34, 35]. They were first discovered as a plasmid-stabilising mechanism [36, 37], and were further shown to possess many functionalities in maintaining genome stability [38], stress responses [35, 39], and pathogenicity [40, 41]. Eight types of toxin-antitoxin systems are currently described with the toxin-antitoxin pairs known to be orthogonal [32, 34, 35, 42]. Among them, the type II mRNA interferase toxins MazF and RelE have been expressed into yeast previously to drive counter selection and inducible growth defects [43, 44]. The toxicity of RelE is antagonised by RelB, and MazF by MazE [44, 45]. In bacteria, tenable copy number systems have traditionally relied on extrachromosomal plasmids [37, 46–48]. In *S. cerevisiae*, titrating the expression ratio of RelE and RelB resulted in varying growth rate [49], which could be exploited as a selection mechanism to modulate tandem-repeat gene integration and gene amplification.

In this study, we investigate the use of the type-II toxin-antitoxin pair, RelE-RelB from *Escherichia coli* (*E. coli*), for driving the selection of tandem-repeat gene amplification. We firstly validate a tri-vector system, showing the multi-copy integration of transgenes occurs independent of RelE-RelB selection. We further show that inducing the expression of toxin RelE causes growth inhibition and further the amplification of the antitoxin RelB-containing module in heterogeneous manners. Evidence from the fluorescent protein reporter and the chromoprotein reporter suggest that the resulted multi-copy integration is unstable in the absence of RelE-driven selection and the stability varies in the strain isolates that have different gene copy number.

Results

Multi-copy chromosome integration independent from toxin-antitoxin selection

We hypothesized that adjusting expression balance between RelE and RelB might be used to generate a selection force to drive gene amplification. For example, if RelE were to be expressed at a relatively high level and RelB was expressed at a relatively low level, there will be a selection pressure for cells to drive the amplification of RelB, as increased gene dosage of RelB may alleviate RelE toxicity.

To test this hypothesis, we designed a three-plasmid genetic system to introduce the expression cassettes of RelE, RelB, a hygromycin B resistant marker (hygromycin B phosphotransferase, Hph), and a yeast-enhanced green fluorescent protein (yEGFP) reporter (Figure 1). To promote gene amplification, the late-firing replication origin (ARS712) was incorporated, which is known to induce replication fork stalling and subsequent repair by break-induced replication, leading to tandem repeat expansion [19, 50]. The expression cassttes of RelE and Hph are closely linked and can be integrated into the yeast chromosome through the homologous recombination targeting to the *HO* locus. The expression cassettes of RelB and yEGFP are closed linked and can be integrated into *HO* promoter region to form two repeated *HO* promoters. In the first design, RelE is under the control of a strong constitutive promoter (the *TDH3* promoter), and RelB is under the control of a medium strong promoter (the *RPL8B* promoter; Supplementary Figure S1). The *TDH3* promoter is ~six-fold stronger than the *RPL8B* promoter [51]. However, the transformation of this contrast was difficult. In one attempt when 5 μg RelB module (linearised pToxAmp1) was transformed, only two large colonies grew with one showing a strong green fluorescence (Supplementary Figure S1). The low transformation efficiency might be as the result of acute toxicity caused by RelE overexpression and the RelB module was not efficiently amplified to rescue the toxicity during the transformation selection process.

In the second design, we used a copper(II)-inducible promoter, the *CUP1* promoter, to control the RelE expression (Figure 1). The *CUP1* promoter exhibits a weak basal activity in the absence of additional copper(II) [51], which may allow the positive selection of the integration of the RelB-yEGFP module. In the presence of additional copper(II) (e.g., 100 μM), the *CUP1* promoter activities can be induced to the levels ~three-fold stronger than the *RPL8B* promoter activities [51]. In theory, this could provide a mechanism to induce RelE expression for selection of the amplification of the RelB-yEGFP module. We transformed strain CEN.PK113-7D with the constructs of this design [52], and transformants were selected on the yeast extract-peptone-dextrose (YPD) hygromycin B plates without copper(II) addition. The fluorescence in most of colonies was not detectable (Figure 1).

Twenty colonies were picked and grown overnight in liquid culture. The resulting yeast cells were collected and washed. Five out of twenty colonies showed green fluorescence (Figure 1). We characterised yEGFP fluorescence using flow cytometry and copy number using quantitative real-time polymerase chain reaction (PCR) in these five colonies and three control colonies that did not show increased fluorescence (Figure 1). Green fluorescence protein (GFP) fluorescence and gene were not present in the control colonies (Figure 1). In the five colonies, the copy number of yEGFP gene ranges from one to ten, and GFP fluorescence was positively correlated with yEGFP gene copy number (R^2 = 0.99; Figure 1; Supplementary Figure S2).

We performed yeast colony PCR to verify the integration of transgenes in the three-plasmid system. In the fluorescent clone A7, the amplification of bands d, and f, indicates the integration of

yEGFP-RelB construct at *HO* promoter locus, the band e for the formation of tandem repeats, and the bands c and f for the integration of the RelE construct (Figure 1A, 1B). Multi-copy integration in clone A7 was confirmed through Oxford nanopore whole genome sequencing (Supplementary Figure S3). In the clone without the yEGFP fluorescence, the amplification of band b indicates the integration of the *RelE* construct (Figure 1A, 1B). This was unexpected. These fluorescent colonies were grown in the YPD medium with addition of 100 μM copper(II) sulfate from a very low OD_{600} (~0.004) and transferred the cultures under the same conditions. The fluorescence levels did not increase. Later, we found that there was a single base pair insertion after the second codon of *RelE* open reading frame (Supplementary Figure S4). This indicates that the toxin *RelE* was not functioning in selection of the multi-copy integration of the yEGFP-RelB construct. Therefore, we presume that the integration of the yEGFP-RelB construct happened as a co-transformation event that coupled with the transformation of the selectable marker Hph and "dead" (inactive)-RelE constructs. Together, these data indicate that multi-copy chromosome integration in these strains does not depend on the toxin-antitoxin selection.

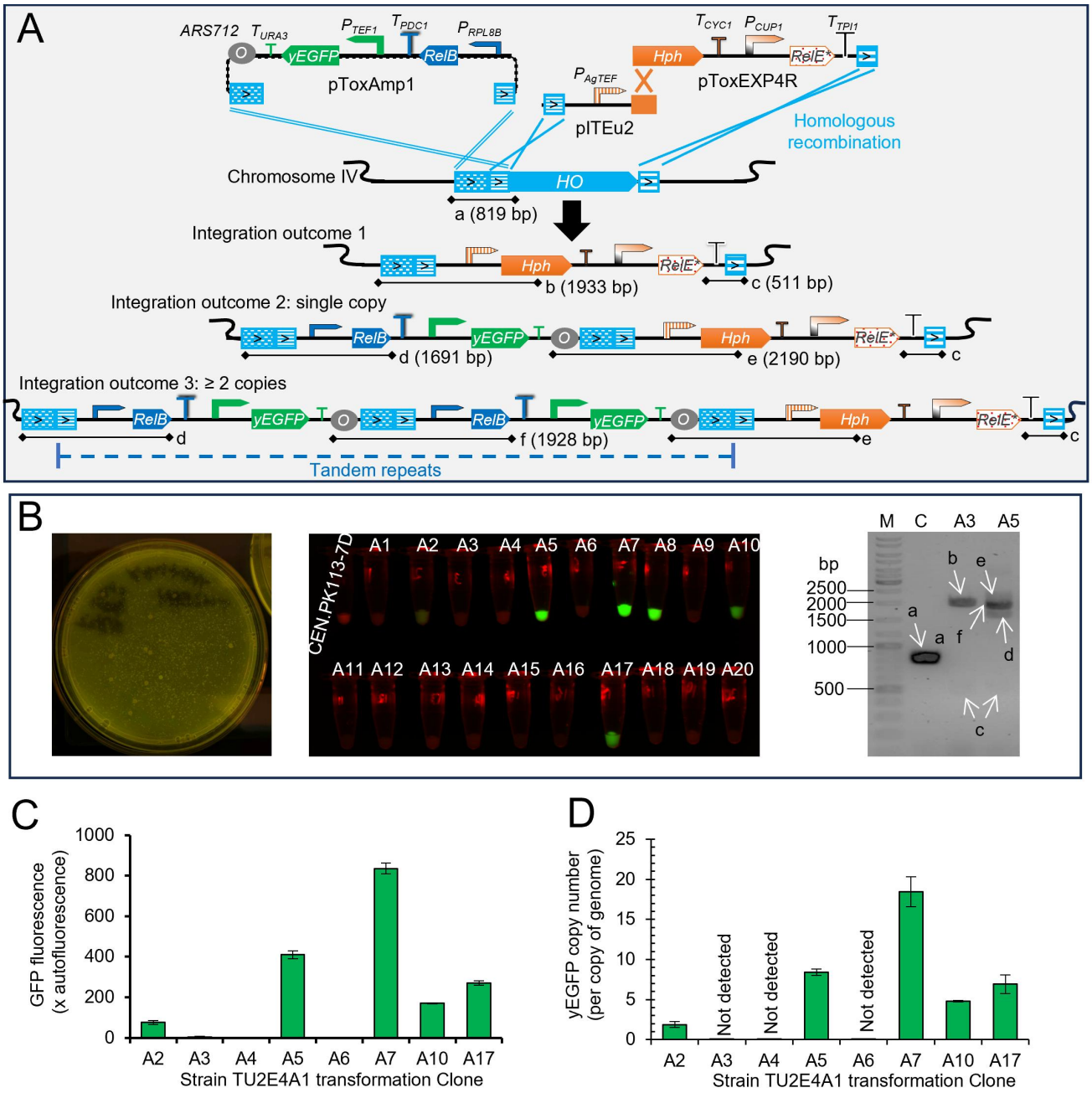

Figure 1 A tri-vector system to deliver the integration of tandem gene repeats, not depending on the functional toxin-antitoxin selection. (A) Diagram of the tri-vector systems and integration outcomes. Fragments from the three vectors: pToxAmp1, pITEu2, and pToxEXP4R. (B) Transformation outcomes for strain TU2E4A1: a transformation plate (diameter: 9 cm) under the blue-light illumination, the yeast cells of isolated clones under blue-light illumination, and colony PCR results. (C & D) yEGFP fluorescence and gene copy numbers in selected clones. Mean value ± standard deviation are shown (n = 3 technical replicates). yEGFP fluorescence was determined using Accuri C6 flowcytometry. a–f, PCR fragments for genotype determination; A1–A20, isolated clone number; ARS712, replication origin; T_{XXXN}, the terminator of XXXN gene; P_{XXXN}, the promoter of XXXN gene; yEGFP, yeast enhanced green fluorescent protein; RelB, antitoxin gene; RelE*, mutated non-functional ('dead') toxin gene; HO, YDL227C gene from *Saccharomyces cerevisiae*; ToxAmp, toxin-antitoxin-mediated gene amplification; M, DNA ladder marker (Thermo Fisher #SM0331, Waltham, MA, USA); C, the control strain CEN.PK113-7D.

Toxin-antitoxin-driven gene amplification

Although the multi-copy chromosome integration does not depend on the toxin-antitoxin selection, it is still interesting to see whether increasing the toxin expression can provide an evolutionary pressure to drive or select the amplification of antitoxin-expressing module. We therefore attempted to reconstruct the plasmid with the *RelE* gene under the control of the *CUP1* promoter but failed to generate a plasmid with the correct sequence. We presume that the *CUP1* promoter might be active in *E. coli*. To solve this problem, we inserted the *RPL28* intron in the middle of the *RelE* gene. We successfully constructed two RelE$_{[RPL28\ intron]}$ constructs: in one, the *CUP1* promoter was used to control RelE expression, and in the other, the *GAL1* promoter was used (Figure 2A).

In the antitoxin RelB-yEGFP module, the *RPL8B* promoter was used to control RelB expression. We also made another RelB-yEGFP constructs, in which the copper-repressible *CTR1* promoter was used to control RelB expression (Figure 2A).

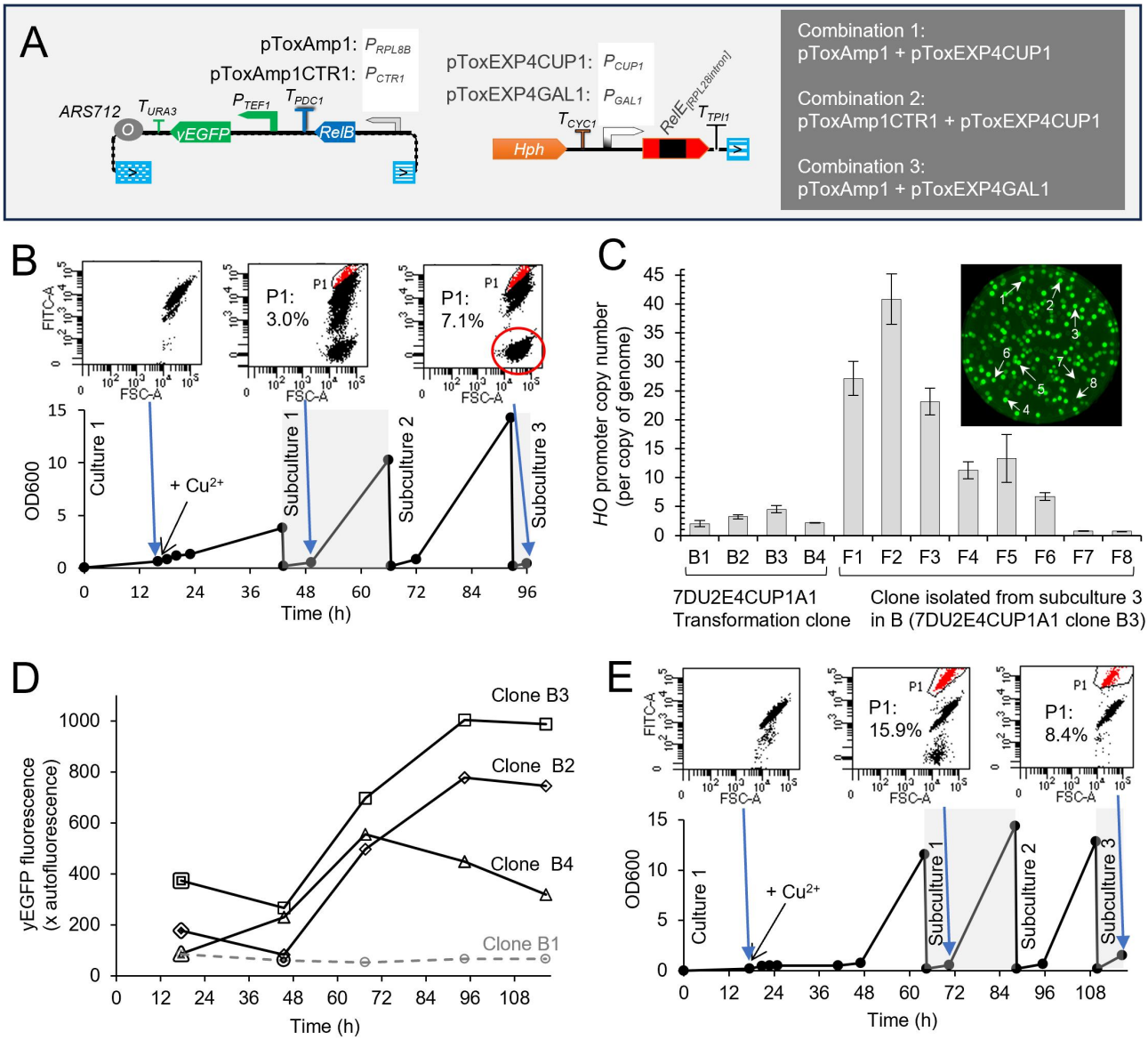

Figure 2 The copper(II)-inducible *in vivo* gene amplification driven by the bacterial type-II toxin-antitoxin (RelE-RelB) pair (ToxAmp).

(A) Plasmids of the tri-vector systems for ToxAmp and the combinations tested. Fragments from the three vectors: pToxAmp1/pToxAmp1CTR1, pJIE13HD7, and pToxEXP4CUP1/pToxEXP4GAL1. (B) The evolutionary effects of copper(II) induction in Combination 1 transformant (7DU2E4CUP1A1) clone B3 (Supplementary Figure S5; the isolate was not pure). (C) *HO* promoter copy numbers in Combination 1 transformants (7DU2E4CUP1A1: B1–B4) and the isolates (F1–F8) from the evolved culture as indicated in the fluorescence image of the culture plate (diameter: 9 cm). (D) Copper(II)-induced evolutionary effects on overall yEGFP fluorescence for the pure Combination 1 transformant isolates (B1–B4). The markers with double lines indicate the starting time of copper(II) induction. (E) Copper(II)-induced evolution for the pure Combination 1 transformation isolate B4, harbouring a single-copy integration of pToxAmp1. P1 (population in red; B & E) indicates the cells with the yEGFP-RelB module amplified. The red circle in B indicates the enriched population of cells without the Combination 1 constructs transformed, as the B3 clone (Supplementary Figure S5) was not grown on the antibiotic-selective plate and was therefore not pure. Synthetic minimal media, yeast nitrogen base wo/amino acids + glucose, were used for yeast cultivation. Copper(II) sulphate of 100 μM was added to induce the evolution. Mean value ± standard deviation were shown (C; n = 3 technical replicates). B & E, FITC PMT voltage = 350. D, n = 1. The details of evolutionary cultivation for pure clones B1–B3 are shown in Supplementary Figure S9. ARS712, replication origin; yEGFP, yeast enhanced green fluorescent protein; RelB, antitoxin gene, RelE$_{[RPL28\ intron]}$, the toxin gene RelE inserted with the *RPL28* intron; *HO*, YDL227C gene from *Saccharomyces cerevisiae*; ToxAmp, toxin-antitoxin-mediated gene amplification; FSC-A, forward-scatter area.

We transformed CEN.PK117-7D with $RelE_{[RPL28\ intron]}$-expressing module and RelB-yEGFP-expressing module in three combinations: P_{CUP1}-RelE with P_{RPL8B}-RelB (Combination 1), P_{CUP1}-RelE with P_{CTR1}-RelB (Combination 2), and P_{GAL1}-RelE with P_{RPL8B}-RelB (Combination 3). Transformants were selected on YPD agar supplemented with hygromycin. Both fluorescent clones and non-fluorescent clones were obtained. Fluorescent clones included bright clones and dim clones (Supplementary Figure S5). Yeast colony PCR results indicate that the dim clones have a single-copy integration of the RelB-yEGFP module, the bright clones have a multi-copy integration, and the non-fluorescent clones have no integration of RelB-yEGFP-expressing module (Supplementary Figure S5).

For each transformation combination, we chose two clones with a single-copy integration and two clones with a multi-copy integration to test whether the induction of toxin RelE expression could drive and select for amplification of the RelB-yEGFP module. For the clones with the P_{CUP1}-RelE and P_{RPL8B}-RelB cassettes (Combination 1), cells were grown in MES-buffered yeast nitrogen base (YNB)-glucose broth with 100 μM copper(II) sulphate. For the clones with the P_{CUP1}-RelE and P_{CTR1}-RelB cassettes (Combination 2), cells were grown in YPD broth with 100 μM copper(II) sulphate, as they did not grow in YNB-glucose broth. For the clones with P_{GAL1}-RelE and P_{RPL8B}-RelB cassettes (Combination 3), the cells were grown in MES-buffered YNB-galactose broth. Only cells with the P_{CUP1}-RelE and P_{RPL8B}-RelB cassettes (Combination 1) had populations with increased yEGFP fluorescence were observed (Figure 2B). In the cells of other Combinations, we did not observe the evolution towards increased yEGFP fluorescence.

We investigated the copy numbers of the Combination 1 (P_{CUP1}-RelE and P_{RPL8B}-RelB) clones before the copper(II)-induced evolution. Consistent with the colony PCR results (Supplementary Figure S5), clone B1 and clone B4 harboured single-copy integration (two copies of *HO* promoters), and clone B2 and clone B3 harboured two or four copies of integration.

We isolated the single colonies from the evolved culture of clone B3. Colonies showing different levels of GFP fluorescence were isolated. The copy number increased up to ~40 copies per copy of genome (Figure 2D). In the clones with very weak green fluorescence, the *HO* promoter copy number was ~one (Figure 2D). Integration of a single copy of the *GFP*-RelB construct resulted in two copies of the *HO* promoter per copy of genome. This indicates a lack of the integration of *GFP*-RelB construct in these clones.

To understand what happened in the cells that lost the fluorescence during evolution, we performed the whole genome sequencing for Combination 1 strain clone B4 (the single-copy integration clone; Supplementary Figure S5) and its evolution culture. Genome assembly confirms the single-copy integration in Combination 1 strain clone B4 (Supplementary Figure S6) and shows the wildtype *HO* (*YDL227C*) locus in the evolution culture (Supplementary Figure S7), indicating a contamination. The contamination was likely caused by a procedural mistake: the colonies picked from the transformation plates were replicated on the YPD agar in the absence of hygromycin selection (Supplementary Figure S5). The sequencing coverage was low for the clone B4 evolution culture sample, which prevented the assembly of the RelE module and the RelB-yEGFP module; but we could find the nanopore reads to confirm their existence and the tandem repeats of RelB-yEGFP module in this sample (Supplementary Figure S8).

To test the evolutionary outcome of the toxin-antitoxin-driven gene amplification, we isolated the single colonies for the clones of Combination 1 and Combination 3 strains and re-performed the copper(II)-induced evolution (Figure 2D, 2E, Supplementary Figure S9, S10). Induction of RelE expression resulted in a population of cells without yEGFP fluorescence, but this population of cells disappeared in the next round of subcultures (Figure 2E, Supplementary Figure S9A–S9C, S10B–S10E: in seven out of eight experiments). The clones without RelB-yEGFP modules may escape from RelE toxicity after prolonged cultivation (Supplementary Figure S9D, S9E, S10F, S10G). Three out of four clones for the Combination 1 strain, two multi-copy integration clones and one single-copy integration clone, showed a copper(II)-induced increase in the yEGFP fluorescence (Figure 2D). One out of four clones for Combination 3 strain, the single-copy integration clone, showed a small population having yEGFP fluorescence increased upon galactose induction of RelE expression (Supplementary Figure S10C: P1, 0.6%).

Fluorescent reporter for stability visualisation of tandem repeat sequences with toxin-antitoxin selection

Copper(II)-mediated induction of RelE expression triggered the toxin-antitoxin-driven gene amplification, which delivered the multi-copy integration of heterologous genes on the chromosome (Figure 2C). This process often occurs during the process of DNA replication and repair [53], but the resulting tandem-repeat structures may not be mitotically stable. We were interested in the stability of the resulting multi-copy integration. Many techniques and statistical methods have been used to characterise the stability of tandem repeats in cells [54, 55]. Characterisation methods include the examination of gene copy number using quantitative real-time PCR (such as in Figure 1D and Figure 2C), the evaluation of selectable marker stability through growth testing, and whole-genome sequencing [13, 28]. However, these methods can only evaluate a limited number of samples. Alternative methods may be used for visualising the evolution trajectory of tandemly repeated gene locus. In our test, we observed that yEGFP fluorescence was well correlated with its gene copy number (Supplementary Figure S2). Therefore, yEGFP fluorescence can be used as a proxy for copy number to examine the stability.

To test the stability, we sequentially sub-cultured the six multi-copy integration clones, isolated after copper(II)-induced gene amplification (Figure 2C: F1–F6). The six clones were continuously sub-cultured in four media: YPD broth, YPD broth supplemented with 100 μM copper(II), YNB-glucose broth, and YNB-glucose broth supplemented with 100 μM copper(II). The stability profiles in YPD broth were not influenced by the presence of copper(II) (Supplementary Figure S11A, S11B & Figure 3A). Clones F1, F2, and F3, harbouring > 20 copies of the integrated region, decreased in the average GFP fluorescence over the subcultivations (Figure 3A). At the population level, the proportion of the cells having high-level GFP fluorescence decreased, and the proportion of the cells having low-level GFP fluorescence increased (Figure 3B). Clones F4, F5, and F6, harbouring 6–15 copies of integration, were relatively stable, but also showed a slow trend towards losing the population of highest-level fluorescent cells (Figure 3A, 3B).

In YNB-glucose broth, the multi-copy integrations showed a better stability than those in YPD or YPD + copper(II) broth (Figure 3A–3D). However, for the clones harbouring > 20 copies of the integration, the proportion of high-level fluorescent cells decreased at a rate similar to those growing in YPD-based broth (Figure 3B and 3D: F1, F2; Supplementary Figure S11C–S11D: F3). For the clones harbouring 6–15 copies of the integration, the cell population did not change dramatically.

In YNB-glucose + copper(II) broth, the population of the cells having > 20 copies of the integration was relatively stable (Figure 3E, 3F; Supplementary Figure S11E). The clones having 6–15 copies of the integration evolved towards increased yEGFP fluorescence, consistently with the toxin-antitoxin-driven gene amplification.

Chromoprotein for stability visualisation of tandem repeat sequences

Using yEGFP as the reporter, we examined the stability of tandem repeat sequences in liquid culture (Figure 3). At the single-colony levels, we also observed the potential instability of yEGFP-expressing cells, shown as the colonies patterned with sectors under blue-light illumination (Supplementary Figure S1). We were interested in developing an educational kit to demonstrate the phenomenon of genetic stability of tandem repeat sequences. For this purpose, a chromoprotein reporter might be better than a fluorescent reporter, since it can be observed with the naked eye. Therefore, we designed and synthesised a pToxAmp12 construct (Figure 4A), in which the yEGFP expression cassette was replaced with an expression cassette of

the blue chromoprotein from *Actinia equina* (AeBlue) [56, 57]. In the AeBlue expression cassette, a strong constitutive *TDH3* promoter and a synthetic mini-terminator (T_{synth7}) were used to control AeBlue expression [58]. However, this experiment was performed before the best construct for the toxin-antitoxin-driven gene amplification was revealed (Figure 2A), hence we used a non-optimal design. We used the constructs with the *RelB* under the control of the *CTR1* promoter (pToxAmp12: Figure 4A) and the construct with the dead-RelE (pToxEXP4R: Figure 1A, Figure 4A). The three constructs were transformed into *S. cerevisiae* strain CEN.PK113-7D. Blue colonies appeared together with the white colonies on the selection plate, indicating the co-transformation of *AeBlue-RelB* construct with the *Hph* and dead-*RelE* constructs.

We isolated four blue clones (Figure 4B. Clones G1, G2, G3, and G4) and two white clones (Figure 4B. Clones G5 and G6). The colony PCR results support the multi-copy integration of the AeBlue-*RelB* construct in the blue clones. We used quantitative PCR to analyse the copy number of the *HO* promoter region that was amplified together with AeBlue and RelB. This further confirmed that the multi-copy integration was not dependent on toxin-antitoxin selection. In the white clones, the *HO* copy number is one, indicating that the AeBlue-RelB construct was not integrated. In the blue clones, the *HO* promoter copy-number ranges from three to six, indicating multi-copy integration of the AeBlue-RelB construct. Oxford Nanopore whole genome sequencing confirmed the three-copy integration of the AeBlue-RelB construct at the *HO* locus in Clone G2 (Supplementary Figure S12). Clone G1 (five-copy integration) shows a darker blue colour than clones G2/G3/G4 (two-copy integration). This suggests that the colour saturation of the yeast colonies correlate with the copy numbers of the AeBlue gene. This allows a direct observation of the stability and variation of AeBlue tandem repeats in prolonged cultivation.

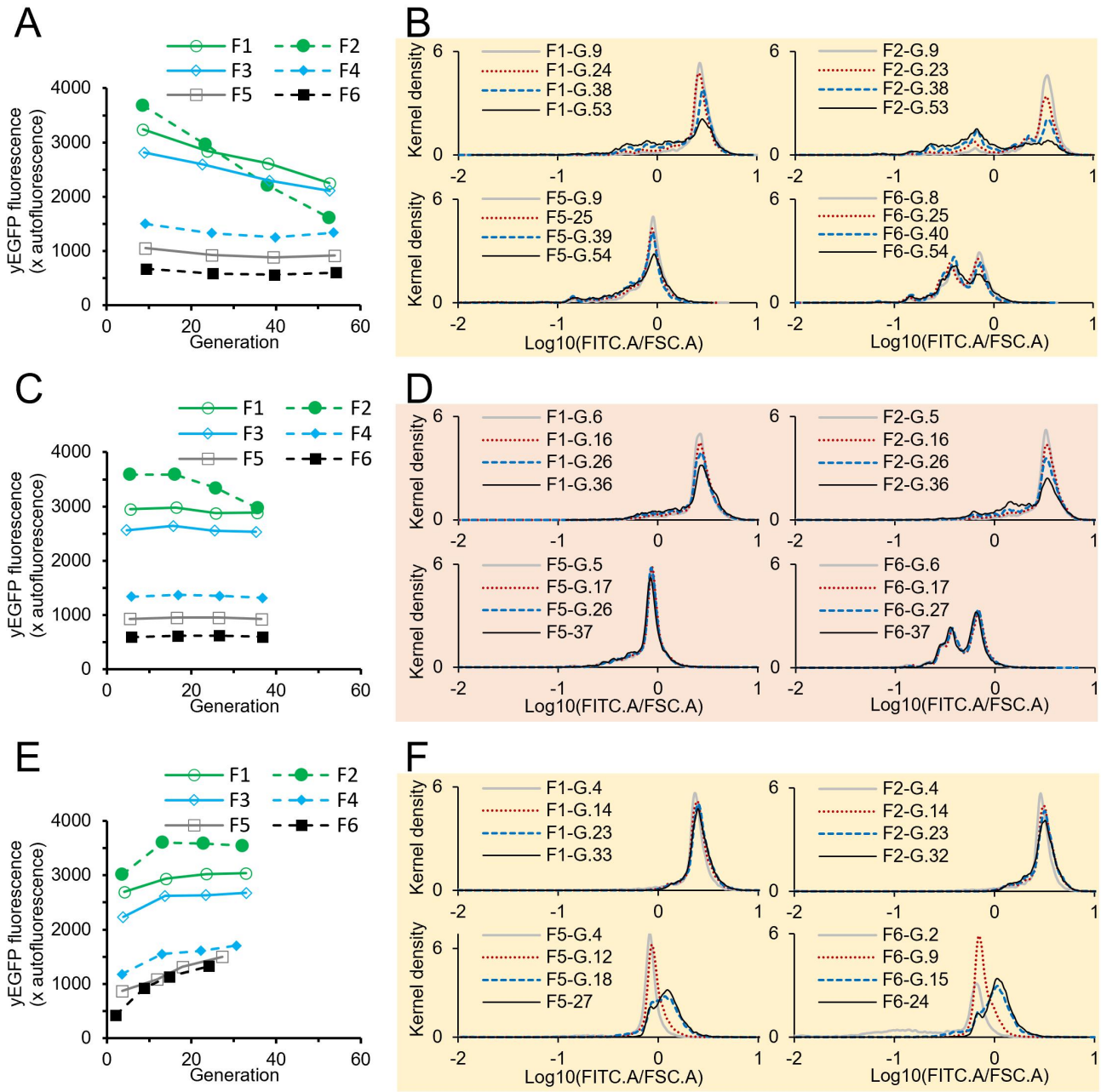

Figure 3 The stability of the multi-copy integration of the yEGFP expression cassettes via the *RelE-RelB*-driven gene amplification. (A & B) YPD broth supplemented with 100 μM copper(II). (C & D) YNB-glucose broth. (E & F) YNB-glucose broth supplemented with 100 μM copper(II). G., generation. A–F, n = 1. The bandwidth of kernel density is 0.01. YPD, yeast extract-peptone-dextrose; YNB, yeast nitrogen base; yEGFP, yeast enhanced green fluorescent protein; FITC.A, fluorescein isothiocyanate area; FSC.A, forward scatter area.

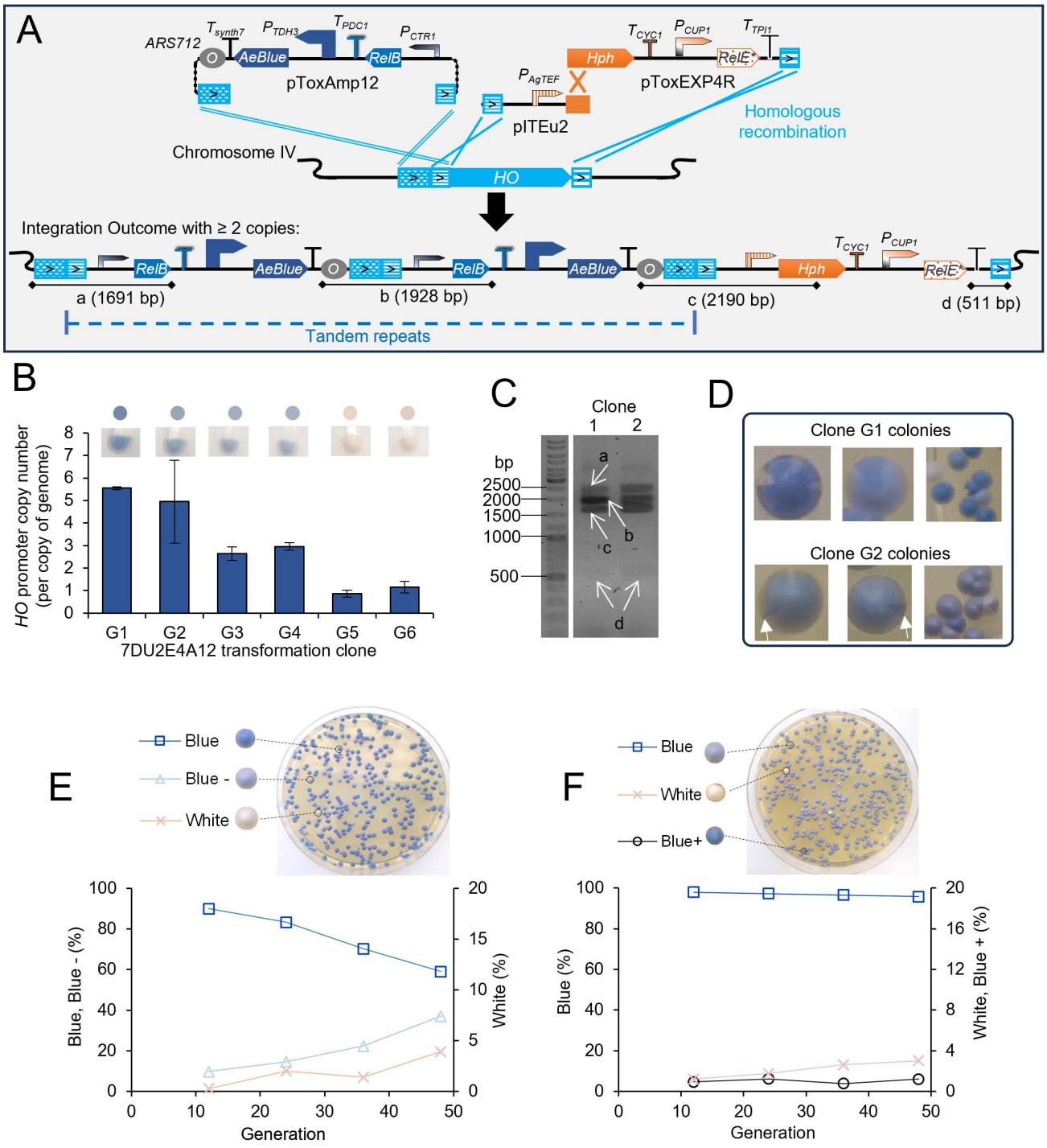

Figure 4 Using AeBlue to visualise the stability of tandem gene repeats in yeast.

(A) Genetic constructs for introduction of multi-copy integration of AeBlue overexpression cassette. (B) *HO* promoter copy number in the yeast clones isolated from transformation plates. The colour of cell pellets is shown above the bars. The dots represent the colour of cell pellets. (C) Yeast colony PCR to verify the integration pattern (bands a, b, c, and d refer to the amplicons shown in A). (D) Single yeast colonies showing the stability of multi-copy integration of AeBlue overexpression cassette. White arrows show the sectors with increased saturation, which means increased copy number. (E & F) Stability analysis via counting the colonies with three-scaled hue in continuous transferring cultivation: G1 (E) and G2 (F). Petri dish diameter: 9 cm. Mean values ± standard deviation are shown in (B) (n = 3 technical replicates). (E & F), n = 1. Blue, the colonies showing the initial blue hue; Blue-, the colonies showing decreased blue hue; Blue+, the colonies showing increased blue hue; White, the colonies appearing in pale white colour; Hph, hygromycin B phosphotransferase; yEGFP, yeast-enhanced green fluorescent protein; AeBlue, Blue chromoprotein from *Actinia equina*; PCR, polymerase chain reaction; ToxAmp, toxin-antitoxin-mediated gene amplification; ARS712, replication origin; RelB, antitoxin gene; *HO*, YDL227C gene from *Saccharomyces cerevisiae*.

We sub-cultured two blue clones (Clone G1 and Clone G2) over ~48 generations. Yeast cells were spread on YPD plates for each cultivation and incubated at room temperature for a week for full development of AuBlue hue. The colonies on the plate did not show a homogenous

blue colour. Clone G1 colonies showed patterned sectors with decreased hue for most cases (Figure 4D). In Clone G2, sectors with increased hue appeared in very few cases (Figure 4D).

To evaluate the strain stability, we counted the colonies into three scales of blue hue (Figure 4E, 4F). For Clone G1, the proportion of the original blue colonies decreased to ~59% over 48 generations, and less-blue colonies (Blue-) and white colonies gradually increased (Figure 4E). For Clone G2, having lower copy number of AeBlue construct and less blue hue than Clone G1, ~96% colonies maintained the parental blue colour and ~1% colonies showed increased blue colour (Blue+). In the Clone G2 subculture, a brown colony appeared on the agar plate. Subsequent characterisation showed that a deficiency of adenine synthesis led to the production of orange dye and the multi-copy integration can be lost in 10% cells after 45-generation sub-cultivation (Supplementary Result S1, Supplementary Figures S13, S14). The mixture of orange pigment and blue pigment may generate the brown colour.

Discussion

To manipulate the tandem gene repeats in *S. cerevisiae*, we developed a bacterial type-II toxin-antitoxin-mediated gene amplification (ToxAmp) method in this work. To the best of our knowledge, this study represents the first application of toxin-antitoxin-mediated selection for manipulating gene copy-numbers in eukaryotic cells. The integration of the tandem-repeat construct does not depend on the toxin-antitoxin-mediated selection. In the ToxAmp method, inducing the expression of toxin RelE can be detrimental, but it can be rescued by an increase in gene dosage of the antitoxin RelB module. Tandem gene repeats are unstable, with spontaneous increases and decreases in copy number. Although toxin–antitoxin systems exert selection pressure that is critical for maintaining high copy numbers, they are insufficient to produce homogeneous cell populations with uniform copy numbers.

Co-transformation of two different plasmids into *S. cerevisiae* was first reported in the 1970s [59]. We have co-transformed four plasmids to complement four auxotrophic selection markers to establish metabolic engineering strains in one step [60]. Co-transformation of an episomal plasmid and a genome-integrating DNA fragment was also reported in the 1980s, but the co-transformation ratios were low (< 2%) [61]. Here, we re-visited the co-transformation event in *S. cerevisiae* through the genome-integrating tri-vector system (Figure 1). The co-transformation efficiency was higher, ~30%, which might be due to the specific design for the homologous fragments (Figure 1). This is consistent with *S. cerevisiae*'s high-capacity of homologous recombination-based *in vivo* DNA assembly, which was first reported in 1980s and only well exploited for large-DNA fragment assembly 20 years later [62–64].

Multi-copy integration methods were previously investigated in *S. cerevisiae*, and other yeasts for applications in metabolic engineering [13, 65, 66]. For example, increasing copy numbers of synthetic pathway genes has been proven an efficient strategy for boosting the production of various heterologous products, including small molecules such as terpenoids and recombinant proteins [13, 67]. Several strategies, including high-concentration antibiotic-based selection and ribosomal DNA or delta-sequence-targeting integration [20, 22, 65, 67–69], have been widely used for this purpose. Recently, we showed that the typical YIp could be used to deliver multi-copy genome integration in the pattern of tandem gene repeats [30]. We note that YIp delivering multi-copy genome integration has been previously reported in 1981 [70]. The current work further confirms that the multi-copy genome integration feature happens during the transformation, and does not depends on a specific selection pressure (Figure 1, Figure 4). These findings may help to leverage engineering capacity to use the existing yeast integrative vectors, which were not originally designed for multi-copy genome integration, to select the multi-copy integration and explore the phenotypic advantages.

Using AeBlue as the reporter, we observed again that gene amplification happened spontaneously, and does not depend on the selection pressure (Figure 4D, 4F). The induction of RelE under the control of the *CUP1* promoter provided the selection to enrich the cells with increased RelB copies (Figure 3, Supplementary Figure S6). But the acute RelE toxicities *via* the expression under the control of the *GAL1* promoter, two-fold stronger than the *CUP1* promoter under inductive conditions [51], caused growth arrest (Supplementary Figure S10). In these cases, other unknown mechanisms were adopted to escape RelE toxicities (Supplementary Figure S10). A recent report showed that spontaneous mutagenesis inactivated RelE selection in *Pseudomonas protegens* and translational pairing between *RelE* and an isoleucine synthetic enzyme, *ilvA,* overcame the selection of inactivation mutations [71]. Consistent with this, reduced ilvA/RelE was found to contribute to a better selection effect. Here, we observed that the basal expression of *RelE* under the control of the *CUP1* promoter was sufficient to cause growth arrest in YNB broth without 100 μM copper(II) supplement (Supplementary Figure 6D, 6F). These data suggest that strong expression is not essential to drive ToxAmp.

The decreasing in population-averaged yEGFP fluorescence and the population of the cells expressing the high-level yEGFP (Figure 3), along with the appearance of the colonies and the colony section showing little or no expression of AeBlue protein (Figure 4), shows that tandem gene repeats were genetically instable. This is consistent with previous observations that tandem gene repeats can be excised via intrachromosomal recombination (loop-out) and subsequently lost from the chromosome during mitotic segregation [72]. In both yEGFP and AeBlue cases, the lower-copy integration was more stable than the higher-copy integration (Figure 3, Figure 4). Meanwhile, selection pressure is important to maintain the stability of high-copy integration. In YPD broth, 100 μM copper(II) was not sufficient to induce the toxin-antitoxin-mediated selection, which might be due to the copper(II)-chelating properties of amino acids [73, 74]. It has been shown that the copper(II) concentration needs to be in the mM range to induce the *CUP1* promoter [75, 76]. In YNB broth, the integration of 6–15 copies can be stably maintained. This might be due to the basal expression of the *CUP1* promoter in YNB media, 50 whereas the *CUP1* promoter is not active in YPD broth without copper(II) addition [76]. In the ToxAmp construct (Figure 2), the *RPL8B* promoter is used to control the expression of antitoxin *RelB*, and the *CUP1* promoter for toxin *RelE*. The strength of the *RPL8B* promoter controlling *RelB* expression is 6.5-fold higher than the basal strength of the *CUP1* promoter [51]. This suggests that the antitoxin should be expressed at the level much stronger than the toxin to reach the proper balance for detoxification. Furthermore, single-cell sequencing and single-cell quantitative PCR can be further employed to quantify gene copy number changes at the single-cell level to improve our understanding of gene copy number stability across different environments.

In summary, we observed the randomness of copy-number change in tandem gene repeats, including copy-number increases and copy-number decreases. The change does not depend on the selection pressure. The current design leverages recent findings that gene amplification is stimulated by transcriptionally active genes (P_{TEF1}-*yEGFP* and P_{RPL8B}-*RelB*) and by incorporation of a late-firing autonomous replicative sequence (ARS712) [19, 50]. In the absence of the selection pressure, the cell population harbouring high-copy-number repeats rapidly collapsed. In contrast, selection pressure could rapidly enrich for the high-copy-number integration at population levels. These observations indicate the challenges in cancer treatment through inhibition on the gene product of oncogenic tandem repeats [77, 78], and the prevention of the relevant human diseases [79], as tandem repeats inevitably occur during natural proliferation processes. The yeast platforms established in this study can be further applied to systematically elucidate the genetic and molecular factors that govern tandem gene repeat stability, with potential applications in treating associated genetic disorders. The AeBlue-expressing ToxAmp constructs provide a eukaryotic system to visualise the trajectories of tandem gene repeats in complement to the *E. coli* system [80], and can be used for educational purposes to demonstrate genetic variations in cell proliferation. Introduction of

stable multi-copy gene integration can be used for optimisation of bioproduction in metabolic engineering [13]. However, the current version of the toxin-antitoxin-mediated gene amplification system does not produce cells with uniform copy numbers. The heterogeneity observed in the engineering outcomes of this system, potentially arising from interactions between the toxin–antitoxin module and endogenous genetic networks, remains unclear. Improved designs as well as other bacterial type-II toxin-antitoxin pairs can be further exploited [32, 34, 81].

Materials and methods

Plasmid and yeast strains

Plasmids and *S. cerevisiae* strains are listed in Supplementary Data File S1. Plasmid sequences are listed in Supplementary Data File S2. Molecular Cloning Designer Simulator was used to simulate plasmid construction [82].

Flow cytometry

Yeast cells were grown in YNB media containing 6.9 g/L yeast nitrogen base without amino acids (YNB, FORMEDIUM; #CYN0402; Hunstanton, England, UK) and 20 g/L glucose to the exponential growth phase (OD_{600} ≤ 2) for characterisation of the yEGFP fluorescence. A BD Accuri™ C6 flow cytometer (BD Biosciences, Franklin Lakes, NJ, USA) was used for fluorescence analysis in single cells (Figure 1). A forward-scatter height threshold of 250,000 was used to exclude cellular debris particles. A 488 nm laser was used to excite GFP fluorescence. The detector equipped with a 530/20 bandpass filter was used to monitor the fluorescence (FL1.A) and 10,000 events were recorded for each sample. BD Csampler software (BD Accuri C6 software version 1.0.264.21) was used to determine mean values of forward-scatter area (FSC.A), side-scatter area (SSC.A) and FL1.A.

A BD FACSCanto II flow cytometer (Firmware version 1.49; BD Biosciences, Franklin Lakes, NJ, USA) was used to measure the yEGFP fluorescence (Figure 2, Figure 3). A 488 nm laser was used to excite the yEGFP fluorescence, and yEGFP fluorescence was monitored at FITC-A channel through a 530/30 nm bandpass filter between two long-pass dichroic mirrors of 556 nm and 502 nm. FITC-A channel PMT voltage was adjusted accordingly to make the FITC-A channel measurement in the range of detection (the value = 300, 350, or 552). A BD FACSDiva™ Software (version 8.0.1; CST Version 3.0.1; PLA version 2.0) was used extract the mean values of FITC-A, forward scatter (FSC-A, PMT voltage = 200; gating threshold = 3,000), and side scatter (SSC-A, PMT voltage = 200).

The fluorescence level of GFP was expressed as the fold of the background fluorescence in CEN.PK 113-7D cells grown to the exponential growth phase according to the previously published equation [51]. To evaluate the kernel density, the data in .fsc file was saved into .csv file using an online converter (https://floreada.io/fcsconvert), and the data were extracted and analysed using R (Supplementary Code 1).

Quantitative real time PCR

NEB Luna® Universal qPCR Master Mix (New England Biolabs, Ipswich, MA, USA) was used, and PCR reactions were prepared in accordance with the manual. Genomic DNA for the reference and experimental samples were diluted with nuclease free water to 0.1 ng/µl and used as templates in quantitative real-time PCR. Primers for quantitative real-time PCR for genes *ACT1*, *yEGFP*, and the *HO* promoter (Supplementary Data 1). Real-time PCR reactions were run in a 384-well plate using a Bio-Rad CFX384™ Touch Real-Time PCR Detection System (Bio-Rad Laboratories, Hercules, CA, USA). SYBR-green fluorophore was used in analysis. Genomic DNA extracted from strain ILHA Y2A-GFP was used for preparing the standard curves and used as the single-copy reference for the yEGFP gene and the *HO* promoter [83]. The gene copy numbers were calculated using the $2^{-\Delta\Delta Ct}$ method [84].

Prolonged transferring cultivation

Induced ToxAmp cultivation. For Combination 1 clones (Figure 2, Supplementary Figure S6), cells were inoculated to OD_{600} of 0.008 in YNB-glucose broth. Copper(II) sulphate was added to a final concentration of 100 µM when OD_{600} was above 0.2. In the following subcultures, YNB-glucose broth supplemented with 100 µM copper(II) sulphate was used and cells were inoculated to OD_{600} of 0.2 to start a new culture. For Combination 2 clones (Figure 2), YPD broth was used instead of YNB-glucose broth. For Combination 3 clones (Figure 2A, Supplementary Figure S5), cells were inoculated to OD_{600} of 0.02 in YNB-glucose broth, grown overnight, washed using water, and inoculated into YNB-galactose broth to OD_{600} of 0.2 to induce ToxAmp. The cells were further sub-cultured in YNB-galactose broth. The yEGFP fluorescence was analysed using A BD FACSCanto II flow cytometer.

Testing the stability of yEGFP-expressing construct. For each subculture, the cells were inoculated to OD_{600} equal to 0.001 for YPD broth and 0.008 for YNB-glucose broth, grown overnight for yEGFP fluorescence measurement when cells were in the exponential growth phase, and grown to 24 h to start a new culture. The yEGFP fluorescence was analysed using A BD FACSCanto II flow cytometer.

Testing the stability of AeBlue-expressing construct. Cells were used to inoculate YPD medium at a concentration of OD_{600} 0.005 and grown in a 200 rpm and 30 °C incubator for 24 h, and the cells were used to start a new culture in the same conditions. For each culture, the cells were diluted to OD_{600}~0.001, and 50 µL of this dilution was spread on YPD agar plates (three plates for each culture). Agar plates were grown in a 30 °C incubator for about 48 h and AeBlue was allowed to mature at room temperature until one week after plates had been spread. Colonies were counted and photographed.

Genome sequencing

Oxford Nanopore whole genome sequencing was performed using the methods described previously [13, 30]. The whole genome DNA was extracted using MagAttract HMW DNA Kit (Qiagen, Venlo, Netherlands) with a modified protocol. A Rapid Barcoding Kit (SQK-RBK114.24, Oxford Nanopore Technologies, Oxford, UK), a R10.4.1 flow cell (FLO-MIN114, Oxford Nanopore Technologies, Oxford, UK), and a MinION sequencing Device (Oxford Nanopore Technologies, Oxford, UK) were used in Nanopore DNA sequencing. A MinKNOW software (23.x, Oxford Nanopore) was used in data collection and base-calling. The .fastq files were merged using a MergeFasta software (DNA BASER, Heracle BioSoft SRL Romania) and deposited in Sequence Read Archive database under submission number SUB14057532. A Canu assembler (Galaxy Version 2.2 + galaxy0), a Maker genome annotation pipeline (Galaxy Version 2.31.11 + galaxy2), and a MiniMap2 (Galaxy Version 2.24 + galaxy0) were used in genome assembly and analysis through a Galaxy server (Galaxy Australia) [85–89]. JBrowse2 (Desktop version v2.6.2) was used to display genetic features [90].

Biosafety and environmental compliance statements

The bacterial toxin RelE is an RNase that is not known to cause disease in plants or animals. Furthermore, the low concentrations of copper(II) sulfate employed in this study pose no significant environmental concerns. All experiments described in this study were conducted in Physical Containment Level 1 or Level 2 facilities in full compliance with Australian regulations.

References

1. Sasaki M, Kobayashi T. Transcription near arrested DNA replication forks triggers ribosomal DNA copy number changes. *Nucl Acids Res.* 2025;53(3):gkaf014. Available at: https://doi.org/10.1093/nar/gkaf014
2. Fan W, Eklund E, Sherman RM, et al. Widespread genetic heterogeneity of human ribosomal RNA genes. *RNA.* 2022;28(4):478–492. Available at: https://doi.org/10.1261/rna.078925.121

3. Hall AN, Morton E, Queitsch C. First discovered, long out of sight, finally visible: ribosomal DNA. *Trends Genet.* 2022;38(6):587–597. Available at: https://doi.org/10.1016/j.tig.2022.02.005
4. Kaushik Tiwari M, Colon-Rios DA, Tumu HCR, et al. Direct targeting of amplified gene loci for proapoptotic anticancer therapy. *Nat Biotechnol.* 2021;40(3):325–334. Available at: https://doi.org/10.1038/s41587-021-01057-5
5. Sandegren L, Andersson DI. Bacterial gene amplification: implications for the evolution of antibiotic resistance. *Nat Rev Microbiol.* 2009;7(8):578–588. Available at: https://doi.org/10.1038/nrmicro2174
6. Domenech P, Kolly GS, Leon-Solis L, Fallow A, Reed MB. Massive gene duplication event among clinical isolates of the Mycobacterium tuberculosis W/Beijing family. *J Bacteriol.* 2010;192(18):4562–4570. Available at: https://doi.org/10.1128/jb.00536-10
7. Powles SB. Gene amplification delivers glyphosate-resistant weed evolution. *Proc Natl Acad Sci USA.* 2010;107(3):955–956. Available at: http://doi.org/10.1073/pnas.0913433107
8. Fierro F, Barredo JL, Díez B, Gutierrez S, Fernández FJ, Martín JF. The penicillin gene cluster is amplified in tandem repeats linked by conserved hexanucleotide sequences. *Proc Natl Acad Sci USA.* 1995;92(13):6200–6204. Available at: https://doi.org/10.1073/pnas.92.13.6200
9. Wang Y, Zhang H, Ri HC, et al. Deletion and tandem duplications of biosynthetic genes drive the diversity of triterpenoids in Aralia elata. *Nat Commun.* 2022;13(1):2224. Available at: http://doi.org/10.1038/s41467-022-29908-y
10. Zhang L, Yu H, Ma B, et al. A natural tandem array alleviates epigenetic repression of IPA1 and leads to superior yielding rice. *Nat Commun.* 2017;8:14789. Available at: https://doi.org/10.1038/ncomms14789
11. He H, Leng Y, Cao X, et al. The pan-tandem repeat map highlights multiallelic variants underlying gene expression and agronomic traits in rice. *Nat Commun.* 2024;15(1):7291. Available at: https://doi.org/10.1038/s41467-024-51854-0
12. Rhie A, Nurk S, Cechova M, et al. The complete sequence of a human Y chromosome. *Nature.* 2023;621(7978):344–354. Available at: https://doi.org/10.1038/s41586-023-06457-y
13. Peng B, Esquirol L, Lu Z, et al. An in vivo gene amplification system for high level expression in *Saccharomyces cerevisiae*. *Nat Commun.* 2022;13(1):2895. Available at: https://doi.org/10.1038/s41467-022-30529-8
14. Tyo KE, Ajikumar PK, Stephanopoulos G. Stabilized gene duplication enables long-term selection-free heterologous pathway expression. *Nat Biotechnol.* 2009;27(8):760–765. Available at: https://doi.org/10.1038/nbt.1555
15. Saleski TE, Chung MT, Carruthers DN, Khasbaatar A, Kurabayashi K, Lin XN. Optimized gene expression from bacterial chromosome by high-throughput integration and screening. *Sci Adv.* 2021;7(7):eabe1767. Available at: https://doi.org/10.1126/sciadv.abe1767
16. Peng P, Wei S. Synthetic engineering of microbes for production of terpenoid food ingredients. *J Agric Food Chem.* 2025;73(17):10052–10068. Available at: https://doi.org/10.1021/acs.jafc.5c01724
17. Peng Q, Huang Z, Sun K, et al. Engineering inducible biomolecular assemblies for genome imaging and manipulation in living cells. *Nat Commun.* 2022;13(1):7933. Available at: https://doi.org/10.1038/s41467-022-35504-x
18. Hotz M, Thayer NH, Hendrickson DG, Schinski EL, Xu J, Gottschling DE. rDNA array length is a major determinant of replicative lifespan in budding yeast. *Proc Natl Acad Sci U S A.* 2022;119(15):e2119593119. Available at: https://doi.org/10.1073/pnas.2119593119
19. Whale AJ, King M, Hull RM, Krueger F, Houseley J. Stimulation of adaptive gene amplification by origin firing under replication fork constraint. *Nucleic Acids Res.* 2022;50(2):915–936. Available at: https://doi.org/10.1093/nar/gkab1257
20. Zheng H, Wang K, Xu X, et al. Highly efficient rDNA-mediated multicopy integration based on the dynamic balance of rDNA in Saccharomyces cerevisiae. *Microb Biotechnol.* 2022;15(5):1511–1524. Available at: https://doi.org/10.1111/1751-7915.14010
21. Lee FWF, Silva NAD. Improved efficiency and stability of multiple cloned gene insertions at the δ sequences of Saccharomyces cerevisiae. *Appl Microbiol Biotechnol.* 1997;48(3):339–345. Available at: https://doi.org/10.1007/s002530051059
22. Semkiv MV, Dmytruk KV, Sibirny AA. Development of a system for multicopy gene integration in Saccharomyces cerevisiae. *J Microbiol Methods.* 2016;120:44–49. Available at: https://doi.org/10.1016/j.mimet.2015.10.023
23. Gnügge R, Rudolf F. Saccharomyces cerevisiae Shuttle vectors. *Yeast.* 2017;34(5):205–221. Available at: https://doi.org/10.1002/yea.3228
24. Yamada R, Taniguchi N, Tanaka T, Ogino C, Fukuda H, Kondo A. Cocktail delta-integration: a novel method to construct cellulolytic enzyme expression ratio-optimized yeast strains. *Microb Cell Fact.* 2010;9:32. Available at: https://doi.org/10.1186/1475-2859-9-32
25. Xu X, Meier F, Blount BA, et al. Trimming the genomic fat: minimising and re-functionalising genomes using synthetic biology. *Nat Commun.* 2023;14(1):1984. Available at: https://doi.org/10.1038/s41467-023-37748-7
26. Moriya H, Shimizu-Yoshida Y, Kitano H. In vivo robustness analysis of cell division cycle genes in *Saccharomyces cerevisiae*. *PLoS Genet.* 2006;2(7):e111. Available at: https://doi.org/10.1371/journal.pgen.0020111
27. Jin YS, Alper H, Yang YT, Stephanopoulos G. Improvement of xylose uptake and ethanol production in recombinant *Saccharomyces cerevisiae* through an inverse metabolic engineering approach. *Appl Environ Microbiol.* 2005;71(12):8249–8256. Available at: https://doi.org/10.1128/AEM.71.12.8249-8256.2005
28. Demeke MM, Foulquié-Moreno MR, Dumortier F, Thevelein JM. Rapid evolution of recombinant *Saccharomyces cerevisiae* for Xylose fermentation through formation of extra-chromosomal circular DNA. *PLoS Genet.* 2015;11(3):e1005010. Available at: https://doi.org/10.1371/journal.pgen.1005010
29. Oh EJ, Skerker JM, Kim SR, et al. Gene Amplification on Demand Accelerates Cellobiose Utilization in Engineered *Saccharomyces cerevisiae*. *Appl Environ Microbiol.* 2016;82(12):3631–3639. Available at: https://doi.org/10.1128/AEM.00410-16
30. Peng B, Weintraub SJ, Lu Z, et al. Integration of Yeast Episomal/Integrative Plasmid Causes Genotypic and Phenotypic Diversity and Improved Sesquiterpene Production in Metabolically Engineered *Saccharomyces cerevisiae*. *ACS Synth Biol.* 2023;13(1):141–156. Available at: http://doi.org/10.1021/acssynbio.3c00363
31. Ni S, Li B, Tang K, et al. Conjugative plasmid-encoded toxin-antitoxin system PrpT/PrpA directly controls plasmid copy number. *Proc Natl Acad Sci U S A.* 2021;118(4):e2011577118. Available at: https://doi.org/10.1073/pnas.2011577118
32. Lin J, Guo Y, Yao J, Tang K, Wang X. Applications of toxin-antitoxin systems in synthetic biology. *Eng Microbiol.* 2023;3(2):100069. Available at: https://doi.org/10.1016/j.engmic.2023.100069
33. Bothfeld WH, Tyo KEJ. Modified bacteria for enhanced

bioproduction and methods of using the same. U.S. Patent US12168679B2. Published December 17, 2024. Available at: https://patents.google.com/patent/US12168679B2/en
34. Jurėnas D, Fraikin N, Goormaghtigh F, Van Melderen L. Biology and evolution of bacterial toxin–antitoxin systems. *Nat Rev Microbiol.* 2022;20(6):335–350. Available at: https://doi.org/10.1038/s41579-021-00661-1
35. Grabe GJ, Giorgio RT, Hall AMJ, et al. Auxiliary interfaces support the evolution of specific toxin–antitoxin pairing. *Nat Chem Biol.* 2021;17(12):1296–1304. Available at: https://doi.org/10.1038/s41589-021-00862-y
36. Gerdes K, Rasmussen PB, Molin S. Unique type of plasmid maintenance function: postsegregational killing of plasmid-free cells. *Proc Natl Acad Sci USA.* 1986;83(10):3116–3120. Available at: https://doi.org/10.1073/pnas.83.10.3116
37. Effe J, Santer M, Wang Y, Feenstra TE, Hülter NF, Dagan T. The combination of active partitioning and toxin-antitoxin systems is most advantageous for low-copy plasmid fitness. *Nat Commun.* 2025;16(1):7078. Available at: https://doi.org/10.1038/s41467-025-62473-8
38. Lefimil C, Bustamante P. Insights into toxin-antitoxin systems in the genus Bifidobacterium. *Appl Environ Microbiol.* 2025;91(12):e0193425. Available at: https://doi.org/10.1128/aem.01934-25
39. Ostyn E, Augagneur Y, Pinel-Marie ML. Insight into the environmental cues modulating the expression of bacterial toxin-antitoxin systems. *FEMS Microbiol Rev.* 2025;49:fuaf007. Available at: https://doi.org/10.1093/femsre/fuaf007
40. Sonika S, Singh S, Mishra S, Verma S. Toxin-antitoxin systems in bacterial pathogenesis. *Heliyon.* 2023;9(4):e14220. Available at: https://doi.org/10.1016/j.heliyon.2023.e14220
41. Maté MJ, Vincentelli R, Foos N, Raoult D, Cambillau C, Ortiz-Lombardía M. Crystal structure of the DNA-bound VapBC2 antitoxin/toxin pair from *Rickettsia felis*. *Nucleic Acids Res.* 2011;40(7):3245–3258. Available at: https://doi.org/10.1093/nar/gkr1167
42. Ding D, Green AG, Wang B, et al. Co-evolution of interacting proteins through non-contacting and non-specific mutations. *Nat Ecol Evol.* 2022;6(5):590–603. Available at: https://doi.org/10.1038/s41559-022-01688-0
43. Yang J, Jiang W, Yang S. mazFas a counter-selectable marker for unmarked genetic modification of *Pichia pastoris*. *FEMS Yeast Res.* 2009;9(4):600–609. Available at: https://doi.org/10.1111/j.1567-1364.2009.00503.x
44. Kristoffersen P, Jensen GB, Gerdes K, Piškur J. Bacterial Toxin-Antitoxin Gene System as Containment Control in Yeast Cells. *Appl Environ Microbiol.* 2000;66(12):5524–5526. Available at: https://doi.org/10.1128/AEM.66.12.5524-5526.2000
45. Alalam H, Sigurdardóttir S, Bourgard C, et al. A Genetic Trap in Yeast for Inhibitors of SARS-CoV-2 Main Protease. *mSystems.* 2021;6(6):e0108721. Available at: https://doi.org/10.1128/mSystems.01087-21
46. Kumar S, Lezia A, Hasty J. Engineering plasmid copy number heterogeneity for dynamic microbial adaptation. *Nat Microbiol.* 2024;9(8):2173–2184. Available at: https://doi.org/10.1038/s41564-024-01706-w
47. Rouches MV, Xu Y, Cortes LBG, Lambert G. A plasmid system with tunable copy number. *Nat Commun.* 2022;13(1):3908. Available at: https://doi.org/10.1038/s41467-022-31422-0
48. Joshi SH, Yong C, Gyorgy A. Inducible plasmid copy number control for synthetic biology in commonly used *E. coli* strains. *Nat Commun.* 2022;13(1):6691. Available at: https://doi.org/10.1038/s41467-022-34390-7
49. Duperray M, François JM, Capp JP. Tuning the expression of the bacterial relBE toxin-antitoxin system in *Saccharomyces cerevisiae* allows characterizing the subsequent growth inhibition. *FEMS Yeast Res.* 2023;23:foad009. Available at: http://doi.org/10.1093/femsyr/foad009
50. Foss EJ, Sripathy S, Gatbonton-Schwager T, et al. Chromosomal Mcm2-7 distribution and the genome replication program in species from yeast to humans. *PLoS Genet.* 2021;17(9):e1009714. Available at: https://doi.org/10.1371/journal.pgen.1009714
51. Peng B, Williams TC, Henry M, Nielsen LK, Vickers CE. Controlling heterologous gene expression in yeast cell factories on different carbon substrates and across the diauxic shift: a comparison of yeast promoter activities. *Microb Cell Fact.* 2015;14:91. Available at: https://doi.org/10.1186/s12934-015-0278-5
52. Entian KD, Kötter P. 25 Yeast Genetic Strain and Plasmid Collections. *Methods Microbiol.* 2007;36:629–666. Available at: https://doi.org/10.1016/S0580-9517(06)36025-4
53. Kovalenko TF, Abdurazakov A, Antipova NV, Shakhparonov MI, Pavlyukov MS. R-loops as a trigger for intra- and extrachromosomal DNA amplification in cancer. *Front Cell Dev Biol.* 2025;13:1647255. Available at: https://doi.org/10.3389/fcell.2025.1647255
54. Dolzhenko E, English A, Dashnow H, et al. Characterization and visualization of tandem repeats at genome scale. *Nat Biotechnol.* 2024;42(10):1606–1614. Available at: https://doi.org/10.1038/s41587-023-02057-3
55. Zhao T, Chiang ZD, Morriss JW, et al. Spatial genomics enables multi-modal study of clonal heterogeneity in tissues. *Nature.* 2021;601(7891):85–91. Available at: https://doi.org/10.1038/s41586-021-04217-4
56. Shkrob MA, Yanushevich YG, Chudakov DM, et al. Far-red fluorescent proteins evolved from a blue chromoprotein from Actinia equina. *Biochem J.* 2005;392(3):649–654. Available at: https://doi.org/10.1042/BJ20051314
57. Ahmed FH, Caputo AT, French NG, et al. Over the rainbow: structural characterization of the chromoproteins gfasPurple, amilCP, spisPink and eforRed. *Acta Crystallogr D Struct Biol.* 2022;78(5):599–612. Available at: https://doi.org/10.1107/S2059798322002625
58. Curran KA, Morse NJ, Markham KA, Wagman AM, Gupta A, Alper HS. Short Synthetic Terminators for Improved Heterologous Gene Expression in Yeast. *ACS Synth Biol.* 2015;4(7):824–832. Available at: https://doi.org/10.1021/sb5003357
59. Hicks JB, Hinnen A, Fink GR. Properties of Yeast Transformation. *Cold Spring Harb Symp Quant Biol.* 1979;43 Pt 2:1305–1313. Available at: https://doi.org/10.1101/sqb.1979.043.01.149
60. Peng B, Plan MR, Chrysanthopoulos P, Hodson MP, Nielsen LK, Vickers CE. A squalene synthase protein degradation method for improved sesquiterpene production in *Saccharomyces cerevisiae*. *Metab Eng.* 2017;39:209–219. Available at: https://doi.org/10.1016/j.ymben.2016.12.003
61. Rudolph H, Koenig-Rauseo I, Hinnen A. One-step gene replacement in yeast by cotransformation. *Gene.* 1985;36(1–2):87–95. Available at: https://doi.org/10.1016/0378-1119(85)90072-1
62. Suzuki K, Imai Y, Yamashita I, Fukui S. In vivo ligation of linear DNA molecules to circular forms in the yeast *Saccharomyces cerevisiae*. *J Bacteriol.* 1983;155(2):747–754. Available at: https://doi.org/10.1128/jb.155.2.747-754.1983
63. Gibson DG, Benders GA, Axelrod KC, et al. One-step assembly in yeast of 25 overlapping DNA fragments to form a complete synthetic *Mycoplasma genitalium* genome. *Proc Natl Acad Sci U S A.* 2008;105(51):20404–20409. Available at: https://doi.org/10.1073/pnas.0811011106
64. Shao Z, Zhao H, Zhao H. DNA assembler, an in vivo genetic method for rapid construction of biochemical pathways. *Nucleic Acids Res.* 2008;37(2):e16. Available at:

https://doi.org/10.1093/nar/gkn991
65. Scorer CA, Clare JJ, McCombie WR, Romanos MA, Sreekrishna K. Rapid Selection Using G418 of High Copy Number Transformants of *Pichia pastoris* for High–level Foreign Gene Expression. *Nat Biotechnol.* 1994;12(2):181–184. Available at: https://doi.org/10.1038/nbt0294-181
66. Lu Z, Evans S, McDonnell L, et al. Exploiting the Geranylgeranyl-Pyrophosphate-Sensing N-Terminal Domain of HMG-CoA Reductase 2 to Regulate Farnesyl Pyrophosphate Synthase (Erg20p) for Improved Monoterpene Production in *Saccharomyces cerevisiae*. *Yeast*. 2025;42:169–180. Available at: https://doi.org/10.1002/yea.4005
67. Lian J, Jin R, Zhao H. Construction of plasmids with tunable copy numbers in *Saccharomyces cerevisiae* and their applications in pathway optimization and multiplex genome integration. *Biotechnol Bioeng.* 2016;113(11):2462–2473. Available at: https://doi.org/10.1002/bit.26004
68. Tokuhiro K, Muramatsu M, Ohto C, et al. Overproduction of Geranylgeraniol by Metabolically Engineered *Saccharomyces cerevisiae*. *Appl Environ Microbiol.* 2009;75(17):5536–5543. Available at: https://doi.org/10.1128/AEM.00277-09
69. Shi S, Liang Y, Zhang MM, Ang EL, Zhao H. A highly efficient single-step, markerless strategy for multi-copy chromosomal integration of large biochemical pathways in *Saccharomyces cerevisiae*. *Metab Eng.* 2016;33:19–27. Available at: https://doi.org/10.1016/j.ymben.2015.10.011
70. Orr-Weaver TL, Szostak JW, Rothstein RJ. Yeast transformation: a model system for the study of recombination. *Proc Natl Acad Sci U S A.* 1981;78(10):6354–6358. Available at: https://doi.org/10.1073/pnas.78.10.6354
71. Chlebek JL, Leonard SP, Kang-Yun C, et al. Prolonging genetic circuit stability through adaptive evolution of overlapping genes. *Nucleic Acids Res.* 2023;51(13):7094–7108. Available at: https://doi.org/10.1093/nar/gkad484
72. Takahashi T, Ogawa M, Koyama Y. Analysis of the Functions of Recombination-Related Genes in the Generation of Large Chromosomal Deletions by Loop-Out Recombination in Aspergillus oryzae. *Eukaryot Cell.* 2012;11(4):507–517. Available at: https://doi.org/10.1128/EC.05208-11
73. Graddon DP, Munday L. Some properties of copper(II) α-amino-acid chelates. *J Inorg Nucl Chem.* 1961;23(3–4):231–244. Available at: https://doi.org/10.1016/0022-1902(61)80250-9
74. Valverde A, Tovar GI, Rio-López NA, et al. Designing Metal-Chelator-like Traps by Encoding Amino Acids in Zirconium-Based Metal–Organic Frameworks. *Chem Mater.* 2022;34(21):9666–9684. Available at: https://doi.org/10.1021/acs.chemmater.2c02431
75. Adamo GM, Brocca S, Passolunghi S, Salvato B, Lotti M. Laboratory evolution of copper tolerant yeast strains. *Microb Cell Fact.* 2012;11:1. Available at: https://doi.org/10.1186/1475-2859-11-1
76. Butt TR, Sternberg EJ, Gorman JA, et al. Copper metallothionein of yeast, structure of the gene, and regulation of expression. *Proc Natl Acad Sci USA.* 1984;81(11):3332–3336. Available at: https://doi.org/10.1073/pnas.81.11.3332
77. Erwin GS, Gürsoy G, Al-Abri R, et al. Recurrent repeat expansions in human cancer genomes. *Nature.* 2023;613(7942):96–102. Available at: https://doi.org/10.1038/s41586-022-05515-1
78. Annapragada AV, Niknafs N, White JR, et al. Genome-wide repeat landscapes in cancer and cell-free DNA. *Sci Transl Med.* 2024;16(738):eadj9283. Available at: https://doi.org/10.1126/scitranslmed.adj9283
79. Trost B, Engchuan W, Nguyen CM, et al. Genome-wide detection of tandem DNA repeats that are expanded in autism. *Nature.* 2020;586(7827):80–86. Available at: https://doi.org/10.1038/s41586-020-2579-z
80. Reams AB, Roth JR. Mechanisms of Gene Duplication and Amplification. *Cold Spring Harb Perspect Biol.* 2015;7(2):a016592. Available at: https://doi.org/10.1101/cshperspect.a016592
81. Bobonis J, Mitosch K, Mateus A, et al. Bacterial retrons encode phage-defending tripartite toxin–antitoxin systems. *Nature.* 2022;609(7925):144–150. Available at: https://doi.org/10.1038/s41586-022-05091-4
82. Shi Z, Vickers CE. Molecular Cloning Designer Simulator (MCDS): All-in-one molecular cloning and genetic engineering design, simulation and management software for complex synthetic biology and metabolic engineering projects. *Metab Eng Commun.* 2016;3:173–186. Available at: https://doi.org/10.1016/j.meteno.2016.05.003
83. Lu Z, Peng B, Ebert BE, Dumsday G, Vickers CE. Auxin-mediated protein depletion for metabolic engineering in terpene-producing yeast. *Nat Commun.* 2021;12(1):1051. Available at: https://doi.org/10.1038/s41467-021-21313-1
84. Livak KJ, Schmittgen TD. Analysis of Relative Gene Expression Data Using Real-Time Quantitative PCR and the $2^{-\Delta\Delta CT}$ Method. *Methods.* 2001;25(4):402–408. Available at: https://doi.org/10.1006/meth.2001.1262
85. Koren S, Walenz BP, Berlin K, Miller JR, Bergman NH, Phillippy AM. Canu: scalable and accurate long-read assembly via adaptive k-mer weighting and repeat separation. *Genome Res.* 2017;27(5):722–736. Available at: https://doi.org/10.1101/gr.215087.116
86. Afgan E, Nekrutenko A, Grüning BA, et al. The Galaxy platform for accessible, reproducible and collaborative biomedical analyses: 2022 update. *Nucleic Acids Res.* 2022;50(W1):W345–W351. Available at: https://doi.org/10.1093/nar/gkac247
87. Campbell MS, Holt C, Moore B, Yandell M. Genome Annotation and Curation Using MAKER and MAKER-P. *Curr Protoc Bioinformatics.* 2014;48:4.11.1–4.11.39. Available at: https://doi.org/10.1002/0471250953.bi0411s48
88. Li H, Durbin R. Fast and accurate long-read alignment with Burrows–Wheeler transform. *Bioinformatics.* 2010;26(5):589–595. Available at: https://doi.org/10.1093/bioinformatics/btp698
89. Li H. Minimap2: pairwise alignment for nucleotide sequences. *Bioinformatics*. 2018;34(18):3094–3100. Available at: https://doi.org/10.1093/bioinformatics/bty191
90. Diesh C, Stevens GJ, Xie P, et al. JBrowse 2: a modular genome browser with views of synteny and structural variation. *Genome Biol.* 2023;24(1):74. Available at: https://doi.org/10.1186/s13059-023-02914-z